Proceedings Paper:

Lizama-Camara, Y.A., Pinna, C. orcid.org/0000-0002-9079-1381, Lu, Z. et al. (1 more author) (2019) Effect of the injection moulding fibre orientation distribution on the fatigue life of short glass fibre reinforced plastics for automotive applications. In: Kerrigan, K., Mativenga, P. and El-Dessouky, H., (eds.) Procedia CIRP. 2nd CIRP Conference on Composite Material Parts Manufacturing, 10-11 Oct 2019, AMRC, Sheffield, UK. Elsevier , pp. 255-260.

https://doi.org/10.1016/j.procir.2019.09.010

Available online at www.sciencedirect.com

ScienceDirect

Procedia CIRP 85 (2019) 252–257

www.elsevier.com/locate/procedia

2nd CIRP Conference on Composite Material Parts Manufacturing (CIRP-CCMPM 2019)

Effect of the injection moulding fibre orientation distribution on the fatigue life of short glass fibre reinforced plastics for automotive applications.

Y.A. Lizama-Camara[a,*], C.Pinna[a], Z. Lu[b], M. Blagdon[b]

[a]*Mechanical Engineering Department, University of Sheffield, 3 Solly St.Sheffield S1 4DF, UK.*
[b]*Jaguar Land Rover Ltd., Abbey Road, Coventry CV3 4LF, UK.*

* Corresponding author. *E-mail address:* yalizamacamara1@sheffield.ac.uk

Abstract

This work presents an analysis of the effect of the fibre orientation distribution on the fatigue life of a 50wt% short glass-fibre reinforced nylon 6,6 composite produced through injection moulding. A multi-stage modelling approach is proposed to predict the fatigue life of specimens cut at various locations in an injection-moulded plaque. Models for injection moulding, material properties prediction, stress distributions in cyclically loaded specimens and fatigue life calculations have been developed and validated by state-of-the-art experimental techniques. Computed tomography was used to characterise the variation of the fibre orientation at a reference location in the plaque, away from the mould's side walls. 3-D Digital Image Correlation was used to quantify full-field strain distributions during mechanical loading. Fatigue testing was performed to generate stress-life (S-N) curves of the material with different fibre orientation distributions. Results showed a highly anisotropic behaviour. Better material performance, in terms of strength, stiffness and fatigue resistance, was observed for specimens aligned with the injection direction. An effect of the proximity of the mould's side walls on fibre alignment was observed with a tensile strength value 20% higher in comparison to that for specimens cut at the reference location. Predicted fatigue lives also improved with higher fibre alignment. Results of the fatigue model validation, at the reference location, showed good agreement between predictions and experimentation, in particular at intermediate lives where a difference of less than 10% was found.

Keywords: Fatigue; Modelling; Fiber reinforced plastic.

1. Introduction

Short fibre reinforced polymer composites are being used more extensively in the automotive industry in load-bearing components. This is in part due to the relatively low cost of the material, the ease of manufacture and the ability of tailoring the material properties. It is also due to the current EU legislation that sets mandatory targets of CO2 emissions for car manufacturers [1].

Field failure of this type of composite materials is mostly due to the cyclic loading conditions seen during duty cycle. In general terms, failure is a product of a statistical distribution of defects [2]. This is caused by a combination of different damage mechanisms [3], that lead to a steady degradation of the mechanical properties. Therefore, a deeper understanding of the fatigue response of this type of materials is needed if they are to be used safely and in a more efficient manner.

The complex microstructure of this type of composites is one of the main challenges as far as the prediction of their fatigue life is concerned. A continuous variation of the fibre orientation distribution through the thickness of the part is indeed usually observed after the injection moulding process. This is clearly identified by a skin-shell-core structure; where fibres are, respectively, more randomly, longitudinally and transversally aligned with respect to the injection direction [4]. Furthermore, the fibre orientation distribution through the thickness also varies within the component as the flow, and therefore the alignment of fibres, is affected by the proximity to the mould's side walls. In the end, this variation of fibre orientation translates into a highly anisotropic material response [5].

10.1016/j.procir.2019.09.010

The present work studies the effect of the injection moulding process on the fatigue behaviour of a short glass-fibre reinforced nylon 6,6 composite. This is done through a multistage modelling procedure aimed at predicting the fatigue life of the material under constant stress amplitude, while minimizing the amount of experimental data needed to calibrate and validate the model. Three different locations were analysed in an injection moulded plaque: a reference area away from the side walls of the mould, a location close to the mould's side edges, and a region near the injection gate. The proposed modelling methodology covers the simulation of the injection moulding process, the prediction of the material mechanical properties, the calculation of stress distributions and the final fatigue life prediction. Finally, the modelling results are validated using state-of-the-art experimental techniques.

2. Experimental work

2.1. Material description

The investigated composite is a nylon 6,6 matrix reinforced with 50wt% short glass-fibres, or PA66GF50. The material was supplied in the form of injection-moulded plaques 150 mm long x150 mm wide x 4 mm thick.

A controlled region close to the centre of the plaque, called Reference, was used to fully characterise the anisotropic material properties (see Fig. 1). Dog bone shaped coupons were cut at 0° (longitudinally), 90° (transversally) and 45° with respect to the flow direction. Only one specimen was machined from each plaque and always at the same location to maintain, as much as possible, consistency in fibre distributions though the thickness of all specimens. Two other additional locations close to the injection gate and to the mould's side edges were used to study the effect of the injection moulding process on the fatigue life of the composite. 0° Edge and 90° Edge oriented specimens were used for this purpose. Figure 1 shows the corresponding locations and orientations of the Reference and Edge specimens with respect to the injection flow direction. Additionally, the humidity content is known to significantly affect the mechanical response of nylon-based plastics [6]. To this effect, and to ensure replicability of the results, the material was brought up to an equivalent humidity level of 23°C and 50%R.H prior to mechanical testing [7]. This translated into a 1 to 1.4% weight of water. The process was done by first drying out the specimens, and then submerging them into a warm-water bath at 55°C. Weight measurements were taken every 24 hrs. Testing was carried out soon after conditioning to reduce the interaction with the atmosphere which could result in loss of water.

2.2. Experimental program

The experimental work started with the characterisation of the material response under quasi-static tensile conditions for all specimens' orientations. Tensile testing was done using a 25kN rated electromechanical Universal Testing Machine, under displacement-controlled conditions at a rate of 2 mm/min. Optical-based digital image correlation (DIC) was used during tensile testing to measure the strain-field evolution at the surface of the specimens. A Correlated Solutions 3D DIC system [8] was used , consisting of two 5 megapixel cameras set at an acquisition rate of one image every 100 milliseconds. The measured strain resolution was 0.01%, with a minimum subset size of 164 μm x 164 μm and a distance between subset centres (step size) of 19 μm.

Fatigue testing was carried out using a 12.5kN rated servo-hydraulic machine with a MOOG SmartTest ONE controller. Testing frequency was set to 5Hz under force-controlled conditions. Three different stress levels and a stress ratio of zero (R=0) were used for these tests. A cut-off limit of 10^6 cycles was set as a fatigue limit. A MTS alignment system was used to minimize the effect of misalignment on the material response. Finally, all testing was conducted at room temperature.

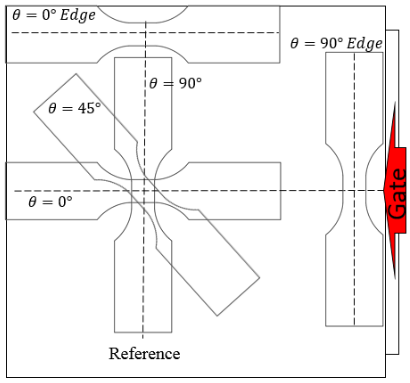

Figure 1 Positions and orientations for Reference and Edge testing specimens.

3. Modelling procedure

3.1. Injection moulding and fibre orientation

The modelling procedure started with the simulation of the injection-moulding process using Autodesk Moldflow [9]. The material's fibre orientation distribution throughout the plaque was predicted in terms of a second order orientation tensor using the Folgar-Tucker fibre orientation model [10]. This tensor is derived from a probability distribution function [11], and represents the probability of fibre alignment along a specific direction. The properties of this tensor are such that the diagonal terms have to be positive and their summation must be equal to 1. Figure 2 shows the results of the injection moulding simulation in terms of the fibre orientation tensor component along the injection direction, or a_{11}. High values (in red) represent fibres more locally aligned with the flow direction. It can be seen from these results that the Reference location corresponds to a uniform region of fibre orientation mostly aligned with the injection flow direction on the top surface of the plaque, and this region was therefore selected to locate the gauge area of the specimens. Significant variations in orientations are observed both in the vicinity of the injection gate, with mid-range fibre orientation values and near the mould's side edges, where alignment with the flow direction is the highest. These two locations were therefore selected to study the effect of proximity with the mould's side walls on the materials' mechanical response.

3.2. Stress analysis

First, a 3D structural finite element mesh of the coupons' geometry was created in Abaqus [12], using reduced integration brick elements with only one Gauss point. The orientation tensor results, from the injection moulding simulation, were then mapped onto the structural mesh via a Node-to-Integration point procedure using Digimat [13]. This was first done by superposing the coupon's mesh to the plaque's mesh. The orientation data from the nodes of the plaque's mesh were then mapped onto the structural mesh's integration points via an interpolation procedure. A convergence study was carried out to select the optimal number of finite elements needed to correctly capture the variation of the fibre orientation tensor through the thickness, with no significant loss of information during the mapping process, while ensuring reasonable computing times. A mesh with 50 elements through the thickness was therefore applied.

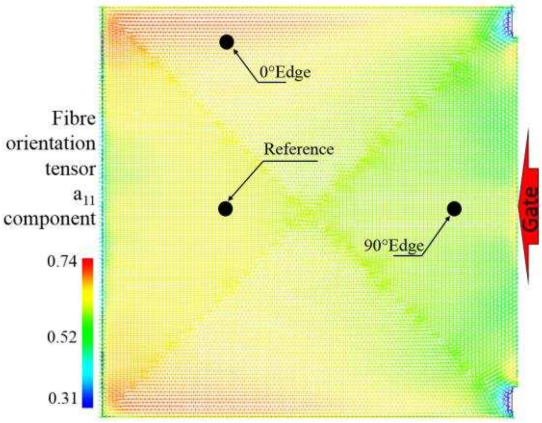

Figure 2 a_{11} fibre orientation tensor component results at the surface of the plaque.

The material properties were calculated using the Mori-Tanaka (M-T) mean-field-homogenization theory using Digimat [13]. This was done through a multi-step homogenization method. The implementation was based on dividing each element in the mesh into several "grains" with similar fibre orientations. Afterwards, the M-T model was applied to calculate homogeneous material properties for each "grain". This allowed to obtain local properties for each element. The material model was first calibrated using PA66 properties for the matrix, obtained from the CAMPUS data base [14]. Textbook elastic properties for type-E glass fibres were used for the reinforcement [15]. This initial material model showed lower levels of strain than the ones measured under tensile testing. Therefore, further refinement was obtained via reverse engineering using experimental data for 0°, 45° and 90° Reference specimens. After calibration of the model (see Figure 7 in results section), elasto-plastic properties were obtained and used as material input for Abaqus to conduct the stress analysis.

To assess the accuracy of the analysis, computed strain results were compared against the DIC strain-field measurements for both the coupon's main and thickness surfaces. Figure 3 shows examples of this comparison for the tensile strain and the maximum principal strain components of a 0° Reference and a 90° Edge specimens, respectively. Strain distributions for both FEA predictions and DIC measurements show a clear strain heterogeneity with localization of deformation at the corners of the gauge length area (through-thickness view), and at the centre of the main surface (main surface view). In Figure 3a comparable strain levels are observed in the central region (in green), where DIC measurements show strain values about 5% higher than in the FEA prediction. However, the DIC measurements show hotspots with strain values 27% higher than those in the FEA results at the same location. In the FE model shown in Figure 3b, strain values are approximately 14% higher in the region at the centre of the gauge area in comparison to the DIC results. Despite these differences, these comparisons show that, for both surfaces, the structural model is capturing the non-homogenous strain distributions expected for this type of composites. This heterogeneous behaviour was also observed for all other specimens' orientations.

3.3. Fatigue analysis

The fatigue modelling was carried out using nCode Design life [16]. The fibre orientation tensor results obtained with Moldflow and stress distributions computed with Abaqus, together with experimental Stress-Life data for the 0° and 90° Reference specimens, were used to calibrate the fatigue model. This was done by using an iterative procedure to reverse engineer S-N curves for fully-aligned longitudinal (along the flow direction), and fully-aligned transversal fibre oriented composites. The Maximum Absolute Principal Stress was used as stress combination method for the fatigue calculation. This model was validated using experimental S-N data for 45° Reference specimens. The validated model at the Reference location was then used to assess the effect of the injection moulding process, especially the effect caused by the proximity of the side walls, by calculating the fatigue life for both Edge specimens at different stress levels.

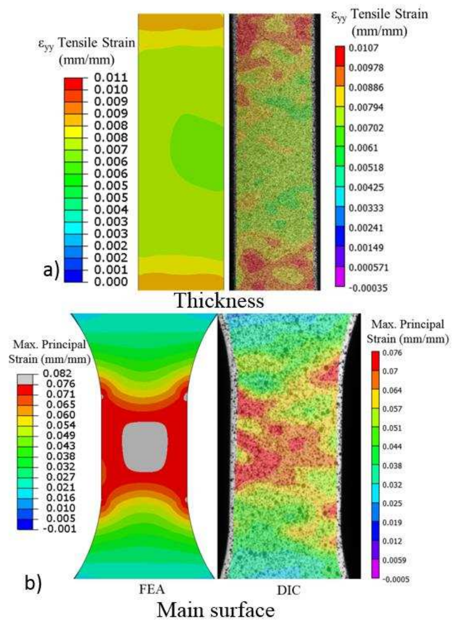

Figure 3 Strain fields comparison for: a) 0° specimen's Tensile Strain through the thickness at 1.6kN; and b) 90°Edge specimen's Max. Principal Strain at 3.5kN on the top main surface. FEA (left) and DIC (right).

4. Results and discussion

4.1. Experimental results

The recorded stress-strain curves corresponding to the Reference and Edge specimens are shown in Figure 4. It can be seen that the tensile behaviour of PA66GF50 shows a clear anisotropic response. At the Reference location, the 0° specimen shows a significant higher stiffness and tensile strength, but also a reduced strain-at-break. The results also show that the curves for 45° and 90° Reference specimens lay very close to each other, with no apparent difference in terms of material stiffness. However, the 45° specimen shows a significant larger strain-at-break in comparison to all other orientations, with a strain value approximately 33% higher than that for the 90° Reference specimen. Similar behaviour has been reported for other polyamide composites in the past [17].

A clear effect of the proximity to the mould's side walls in the injection moulding process is also seen for the 0° Edge specimen, showing a higher stress-at-break, despite similar strain levels to those seen at the Reference location for the 0º specimen. This result could be explained by the higher proportion of fibres aligned with the injection flow direction near the mould's side edges as seen in Figure 2. In contrast, the 90° Edge specimen shows no significant difference with respect to the 90° and 45° Reference specimens, in terms of material stiffness. A slightly larger strain-at-break was observed for this coupon in comparison to the 90° Reference specimen..

Experimental fatigue results in the form of Stress-Life (S-N) curves are shown in Figure 5 for the three different Reference specimen orientations. The effect of the anisotropic fibre distribution in the overall composite's fatigue performance can be seen. Coupons aligned with the injection flow direction (0° Reference) show a significantly higher fatigue life in comparison to the other two orientations. Low scatter between repeats was also observed on these specimens. Additionally, 45° Reference specimens show a relatively higher fatigue life compared to those for the 90° Reference samples. This was in line with the higher toughness response observed for these coupons under quasi-static tensile conditions. Similar behaviour for PA66GF50 has been observed in the past [18].

4.2. Modelling results

The results from the injection moulding simulation in the form of the a_{11} tensor component are shown in Figure 6. These results are compared to computed tomography (CT) measurements taken at the Reference location using a phoenix nanotom nanoCT scanner. Good agreement with experimental values is obtained at the Reference location, for the skin and shell layers with a maximum difference of 5% between the predictions and the measurements. A larger difference is seen for the core layer, where the CT data show a 46% smaller tensor component value compared to that of the simulation result at the Reference location. This is a well-known weakness of the pure F-T flow model. This dissimilarity has been observed to be independent of the material thickness and flow [19]. A very close correlation between the Reference location and the 90° Edge predictions is also seen, with a slight difference at the centre of the plaque and at the surface. In contrast, the prediction for 0° Edge shows very little change in terms of fibre orientation, with an almost constant value through the thickness.

Good agreement was also obtained between the experimental Stress-Strain curves and the predicted material response, as shown in Figure 7. No significant difference was seen between the 45°, 90° Reference and 90° Edge samples, with a close overlapping of the experimental data and the predicted results. A divergence was observed between 0° Reference and 0° Edge samples around 50 to 60MPa, where the material model predicted larger strains than those seen in the experimental results. This is close to the calculated 0.2% Yield strength values for 0° Reference and 0° Edge samples, 47MPa and 55MPa respectively. This suggests that the material model under-estimates strain hardening for specimens more aligned with the flow direction, where the reinforcement could have had a higher effect on the material response than the resin.

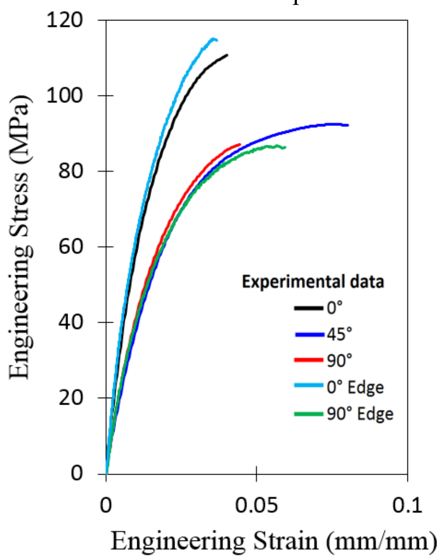

Figure 4 Experimental Stress-Strain curves for PA66GF50 at different locations and orientations.

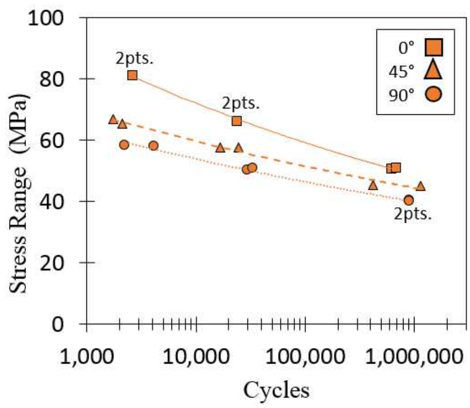

Figure 5 Experimental Stress-Life (S-N) curves for PA66GF50 at R=0.

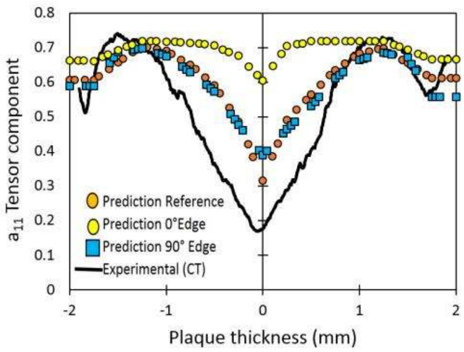

Figure 6 Orientation tensor comparison between Moldflow prediction and computed tomography (CT) measurements.

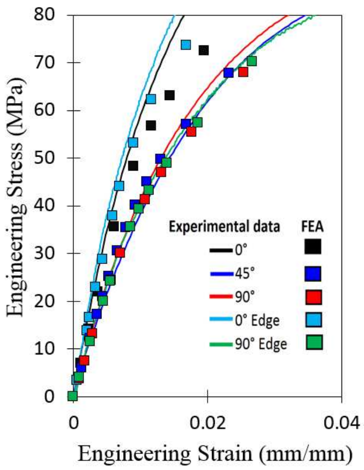

Figure 7 Stress-Strain curves comparison between experimentation and prediction (FEA). Material model calibrated using Reference 0°, 90° and 45° specimens.

Predicted reverse-engineered fully-aligned fatigue curves are shown in Figure 8. The 0° fully-aligned curve shows a higher fatigue life than the rest of the data, Edge specimens included. In contrast, the 90° reverse-engineered fully-aligned curve shows the lowest fatigue life. Predicted fatigue lives for 90° Edge specimens were close to the experimental results for the 90° Reference coupons, with no clear difference between the two locations in the plaque. Predicted 0° Edge specimen results showed better fatigue performance than 0° Reference specimens. This suggests a positive effect with the reinforcement more consistently aligned with the flow direction, as shown in Figure 6.

Finally, the validation of the fatigue model at the Reference location is shown in Figure 9. Predicted lives for 45° Reference specimens shows very good agreement with the Experimental data, with less than 10% difference at intermediate lives.

5. Conclusions

This work proposed a multi-stage model methodology for the fatigue prediction of short fibre reinforced polymers capable of producing reliable results, while requiring a minimum amount of experimentation. The fatigue life of PA66GF50 was found to be highly dependent on the fibre orientation distribution generated during the injection moulding process.

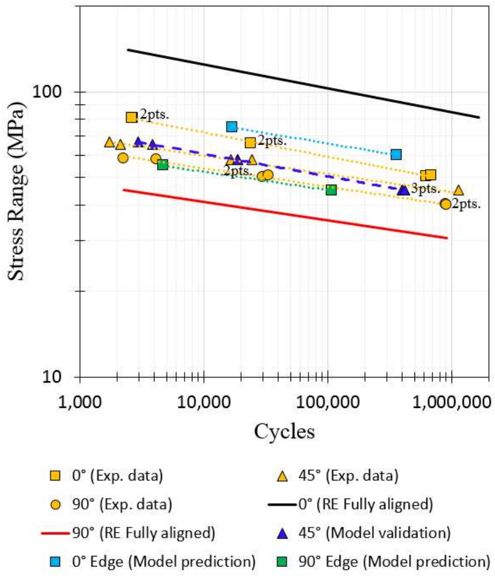

Figure 8 S-N curve comparison between experimental results and life predictions for Reference and Edge specimens.

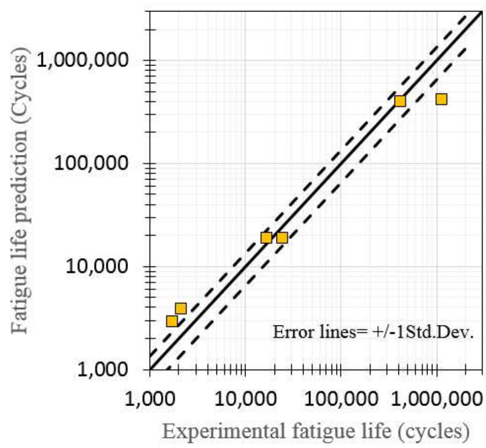

Figure 9 Fatigue results for 45° Reference specimens.

Modelling results showed sensible predictions for the injection moulding simulation and for the stress analyses, capturing the heterogeneous behaviour typical of this type of composites. CT measurements taken at the reference location showed that the model estimated a more random distribution of the fibres in the core region. The comparison of strains fields between FEA and DIC results showed a clear heterogeneous response. Localization of strain was seen in the DIC results in the form of hotspots through the thickness and main surface of the samples. Despite some differences between computed and experimental strain values which might arise, in part, from errors propagated from Moldflow simulations, fatigue prediction has been shown to be very close to the experimental fatigue lives.

Additionally, the injection moulding process seemed to have an effect on both: the tensile and fatigue performance of this type of composites. The fibre alignment was influenced by the closeness to the mould's side edges with an almost constant fibre orientation through the thickness. This effect translated into overall higher tensile strengths and higher predicted fatigue lives than for the Reference location. In contrast, the material performance of specimens taken from regions close to the injection gate showed no significant difference with respect to Reference location specimens.

This work has shown that both the tensile and fatigue properties of these composites vary with the location in injection-moulded parts. The multi-stage modelling approach developed in this work, which takes into account the effect local fibre orientations, has shown very promising results. Further validation is, however, needed by conducting additional tests, especially under more complex loading conditions to demonstrate the performance of the model for automotive applications.

Acknowledgements

The authors would like to acknowledge the Mexican government, through CONACyT, for sponsoring Y.A. Lizama Camara and Jaguar Land Rover for partially funding this project. Additional acknowledgements go to BASF for their material and technical support and, to Autodesk (Moldflow), HBM Prenscia (nCode) and e-Xtream (Digimat) for the support provided in the use of their software.

References

[1] "Regulation (EU) No 333/2014 of the European Parliament and of the Council of 11 March 2014 amending Regulation (EC) No 443/2009 to define the modalities for reaching the 2020 target to reduce CO2 emissions from new passenger cars," *Off. J. Eur. Union*, vol. 57, pp. 15–21, 2014.

[2] Y. K. Lin and J. N. Yang, "A stochastic theory of fatigue crack propagation," *AIAA J.*, vol. 23, no. 1, pp. 117–124, 1985.

[3] E. Belmonte, M. De Monte, C. J. Hoffmann, and M. Quaresimin, "Damage mechanisms in a short glass fiber reinforced polyamide under fatigue loading," *Int. J. Fatigue*, vol. 94, pp. 145–157, 2017.

[4] F. O'Dowd, M. Lévesque, and M. D. Gilchrist, "Analysis of fibre orientation effects on injection moulded components," *Proc. Inst. Mech. Eng. Part B J. Eng. Manuf.*, vol. 220, no. 12, pp. 1909–1921, 2006.

[5] S. Mortazavian and A. Fatemi, "Tensile and fatigue behaviors of polymers for automotive applications," *Materwiss. Werksttech.*, vol. 46, no. 2, pp. 204–213, 2015.

[6] I. Carrascal, J. A. Casado, J. A. Polanco, and F. Gutiérrez-Solana, "Absorption and diffusion of humidity in fiberglass-reinforced polyamide," *Polym. Compos.*, vol. 26, no. 5, pp. 580–586, 2005.

[7] BS EN ISO, *Plastics — Determination of tensile properties Part 1: General principles*. 2012, pp. 1–32.

[8] Correlated Solutions, "Correlated Solutions," 2019. [Online]. Available: https://www.correlatedsolutions.com/. [Accessed: 26-Aug-2019].

[9] Autodesk, "Moldflow Insight 2017." .

[10] F. Folgar and C. L. T. III, "Orientation behaviour of fibers in concentrated suspensions," *J. Reinf. Plast. Compos.*, vol. 3, no. April 1984, pp. 98–119, 1984.

[11] C. Eberhardt and A. Clarke, "Fibre-orientation measurements in short-glass-fibre composites. Part I: Automated, high-angular-resolution measurement by confocal microscopy," *Compos. Sci. Technol.*, vol. 61, no. 10, pp. 1389–1400, 2001.

[12] Dassault Systemes, "Abaqus 6.14-2." .

[13] e-Xstream engineering, "Digimat 2018.1." .

[14] CWFG mbH, "CAMPUS - a material information system for the plastics industry," 2019. [Online]. Available: https://www.campusplastics.com/campus/about. [Accessed: 10-Jun-2019].

[15] F. T. Wallenberger, J. C. Watson, and L. Hong, "Glass Fibers," *ASM Hanb.*, vol. 21, no. Ref 19, pp. 27–34, 2001.

[16] HBM Prenscia, "nCode 2018.1." .

[17] S. Mortazavian and A. Fatemi, "Effects of fiber orientation and anisotropy on tensile strength and elastic modulus of short fiber reinforced polymer composites," *Compos. Part B Eng.*, vol. 72, pp. 116–129, 2015.

[18] P. Wilson and P. Heyes, "Fatigue of short fibre reinforced polymers: from material process to fatigue life of industrial components," in *MATEC Web Conf. 12th International Fatigue Congress (FATIGUE 2018)* ., 2018, vol. 165.

[19] G. Gsellmann, M. Jerabek, and D. Salaberger, "Comparison of predicted and measured fiber orientations in injection molded parts," *Proc. 6th Conf. Ind. Comput. Tomogr.*, 2016.